Theor Appl Climatol (2012) 110:437–456
DOI 10.1007/s00704-012-0633-y

ORIGINAL PAPER

Seasonal climate hindcasts with Eta model nested in CPTEC coupled ocean–atmosphere general circulation model

Isabel L. Pilotto · Sin Chan Chou · Paulo Nobre

Received: 7 June 2011 / Accepted: 8 March 2012 / Published online: 5 April 2012

Abstract This work evaluates the added value of the downscaling technique employed with the Eta model nested in the CPTEC atmospheric general circulation model and in the CPTEC coupled ocean–atmosphere general circulation model (CGCM). The focus is on the austral summer season, December–January–February, with three members each year. Precipitation, latent heat flux, and shortwave radiation flux at the surface hindcast by the models are compared with observational data and model analyses. The global models generally overestimate the precipitation over South America and tropical Atlantic. The CGCM and the nested Eta (Eta + C) both produce a split in the ITCZ precipitation band. The Eta + C produces better precipitation pattern for the studied season. The Eta model reduces the excessive latent heat flux generated by these global models, in particular the Eta + C. Comparison against PIRATA buoys data shows that the Eta + C results in the smallest precipitation and shortwave radiation forecast errors. The Eta + C comparatively best results are though as a consequence of both: the regional model resolution/physics and smaller errors on the lateral boundary conditions provided by the CGCM.

1 Introduction

Regional climate models (RCMs) have become useful tools to simulate climate at higher resolution with reduced computational cost in comparison with the global models. These models have the advantage of representing a more detailed regional characteristics and surface topography and feedback processes with less computational demand. However, studies indicate that regional models are sensitive to the type of nesting strategy (Nobre et al. 2001; Dimitrijevic and Laprise 2005), the choice of the domain area and spatial resolution (Dimitrijevic and Laprise 2005; Antic et al. 2006), and also the data and the resolution of lateral boundary conditions (Druyan et al. 2002; Seth et al. 2007; Amengual et al. 2007; Laprise et al. 2008). On the other hand, lower boundary conditions provided by slowly varying tropical sea surface temperature (SST) have strong effects in the tropical climate (Shukla 1981).

The Eta model has been used for studying seasonal climate in various works adopting continental scale domains and driven by atmospheric global models (e.g., Fennessy and Shukla 2000; Altshuler et al. 2002; Katsafados et al. 2005; Chou et al. 2005). Chou et al. (2000) carried out a 1-month simulation of the rainy season over South America (November 1997) using the Eta model with 80-km resolution nested in the T62L28 CPTEC (The Brazilian Center for Weather Forecasts and Climate Studies) AGCM. The authors found that in general the Eta model improved the representation of the precipitation over the driver AGCM, except in regions of the northeast of Brazil and part of the Amazon. In Chou et al. (2005), precipitation evaluation of 4.5-month Eta model hindcasts for the year 2002 at 40-km resolution showed that the model nested in the CPTEC AGCM represents well the pattern and magnitude of the seasonal precipitation over South America. Multidecadal version of the Eta model was developed (Pesquero et al. 2010) and applied to study the climate of South America in the period between 1961 and 1970 nested in the HadAM3P AGCM from UK Hadley Centre (Pope et al. 2000). Their results at 40-km resolution showed reduction of the bias present in the driver AGCM. A four-member ensemble with the Eta model nested in the HadCM3 CGCM was also

I. L. Pilotto (✉) · S. C. Chou · P. Nobre
National Institute for Space Research—INPE,
Rod. Pres. Dutra km 39,
Cachoeira Paulista, SP, Brazil 12630-000
e-mail: isabel.pilotto@cptec.inpe.br

realized for the present climate considering the period between 1961 and 1990 (Chou et al. 2011). The nested runs produced spread and errors of magnitude comparable to the CGCM runs, but improved the precipitation especially over the Amazon region.

In general regional models applied over South America showed improvement of the simulations over the driver global models by using the downscaling technique (Nobre et al. 2001; Druyan et al. 2002; Misra et al. 2003; Rauscher et al. 2007; Solman et al. 2008). Most of these works used reanalysis or atmospheric global models to drive the RCMs. In this work, the Eta model will be nested in the CGCM and the comparison with the run nested in AGCM will be carried out in the domain covering the tropical Atlantic Ocean.

Coupled ocean–atmosphere global models are the appropriate tools to study the climate variability. On the other hand, these models tend to exhibit some persistent systematic errors such as the double Intertropical Convergence Zone (ITCZ), the warm bias of SST over the southeast Atlantic region or the heat and moisture fluxes, which in some circumstances can severely hinder the CGCM ability to predict seasonal climate variations a few months ahead (Nobre et al. 2006). The atmospheric component has been accounted for some of these errors (e.g., Schneider 2002; Lin 2007). Some works have shown that changes in the ACGM, such as in the horizontal and vertical resolutions (Mechoso 2006), cumulus parameterization scheme (Frey et al. 1997; Zhang and Wang 2006) or formulation of the surface wind stress (Luo et al. 2005), can reduce these errors. Huang et al. (2007) found SST warm bias over the southeast tropical Atlantic which persisted for the 9-month length integrations of the climate forecast system (CFS) of the National Centers for Environmental Prediction (NCEP) for the period from 1981 to 2003. They showed that these errors grew faster during summer and spring, peaking in November and December at about 2 °C. Nobre et al. (2006, 2012) compared the CPTEC AGCM and CGCM, and showed that CGCM improved the precipitation forecasts over the Atlantic Ocean and southeast South America.

In order to validate modeling studies and to identify model systematic errors, observational dataset is necessary; however, the availability of these observations in South America and over the ocean is a restriction to validation works. Reanalysis data is used as an alternative to observations. Over the tropical Atlantic Ocean, the PIRATA (Pilot Research Moored Array in the tropical Atlantic) Project (Bourlès et al. 2008) has provided some buoys measurement.

The objective of this work is to verify the added value of nesting the Eta regional climate model in the CPTEC CGCM to hindcast precipitation, latent heat flux, and shortwave radiation over the tropical Atlantic and South America regions and compare with the model nested in the same global model, but only the atmospheric component. Verification using PIRATA observations will be performed. The data and models are described in Section 2. Section 3 presents the four-way model output comparisons, the validation against the PIRATA buoys, and an evaluation of the ensemble spread. Some conclusions are drawn in Section 4.

2 Data and methodology

2.1 Global models

The CPTEC AGCM, described in detail by Cavalcanti et al. (2002), is a primitive equation spectral model with triangular truncation at wave number 62 and 28 sigma levels unevenly spaced (T062L28). It uses SSiB (Xue et al. 1991) to compute surface fluxes over the continents and a bulk formula over the oceans. The planetary boundary layer closure scheme is that of Mellor and Yamada 2.0 (Mellor and Yamada 1982). The cumulus convection is parameterized by the Kuo scheme (Kuo 1974). The shortwave radiation scheme is based on Lacis and Hansen (1974) and the long-wave radiation scheme is from Harshvardhan et al. (1987). The atmospheric component of the CPTEC CGCM (Nobre et al. 2009) has the same configuration of the CPTEC AGCM, except for the deep convection scheme, which was replaced by the Relaxed Arakawa-Schubert (RAS) scheme (Moorthi and Suarez 1992). The oceanic component uses the Modular Ocean Model version 3 (MOM3) (Pacanowski and Griffies 1998), which was configured in a global tropics grid between 40° S and 40° N, with 1/4×1/4 of a degree latitude–longitude over the tropical Atlantic between 10° S and 10° N, relaxing to a coarser grid over the Pacific and Indian Oceans and extratropics. For the vertical resolution, 20 levels were adopted, seven of them in the first 100 m, spaced by 15 m.

2.2 Regional climate model

The Eta model is a grid-point model and has the feature of the Eta vertical coordinate (Mesinger 1984). The vertical coordinate is approximately horizontal near topography which is an advantage in continent with the steep orography of the Andes Cordillera. The model was setup with 40-km horizontal resolution and 38 vertical layers in hydrostatic mode. The cumulus convection is parameterized by the Betts–Miller–Janjic scheme (Janjic 1994) and the cloud microphysics represented by the Ferrier scheme (Ferrier et al. 2002). The radiation scheme was developed by the Geophysical Fluid Dynamics Laboratory, the shortwave (Lacis and Hansen 1974) and long-wave (Fels and Schwarzkopf 1975) radiation schemes update temperature tendencies every 1 h. The Noah is the land-surface

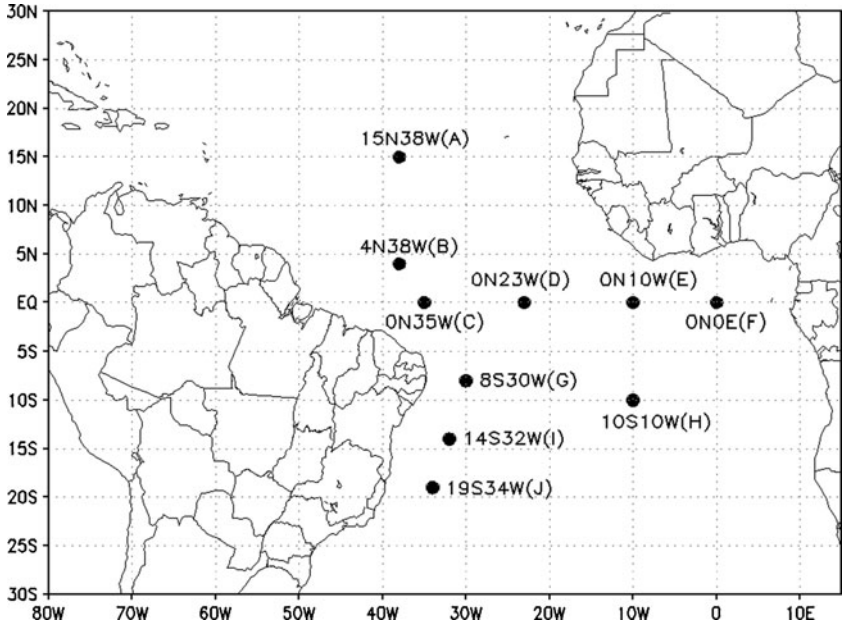

Fig. 1 Position of PIRATA buoys used in the evaluation. The *capital letters A–J* identify the buoy stations

scheme (Ek et al. 2003). In the surface layer, Monin–Obukhov similarity theory is applied with Paulson's function (1970) over the land and Lobocki (1993) functions over the sea with a viscous sublayer (Janjic 1994). The model has been applied for seasonal forecasts at CPTEC since 2003 and evaluation of the seasonal precipitation forecasts can be found in Chou et al. (2005).

2.3 The runs

Two types of nested runs were setup: the Eta model nested in the CPTEC AGCM (Eta + A) and nested in the CPTEC CGCM (Eta + C). The limited area model domain spans from 80° W to 15° E, and 30° S to 30° N, which includes the tropical South America, western Africa, and the tropical Atlantic Ocean.

The season chosen for the study is the austral summer, the months of December, January, and February (DJF). This is the rainy season over the central and southeastern Brazil, when over 50 % of the total annual precipitation occurs (Rao and Hada 1990). Approximately 15 days of atmospheric component spin-up time was included in the runs. In order to generate some spread of the results, an ensemble of three members were constructed. Therefore the integrations started at 1200 UTC, on the days 16, 17, and 18 of November of each year and ended on the last day of February. Ten austral summers were considered in the period of 1997 until 2006. Hence, the AGCM carried out 30 integrations using persisted SST anomaly of November, whereas the CGCM carried out 30 integrations using forecasted SST. The observed SST anomalies are produced and

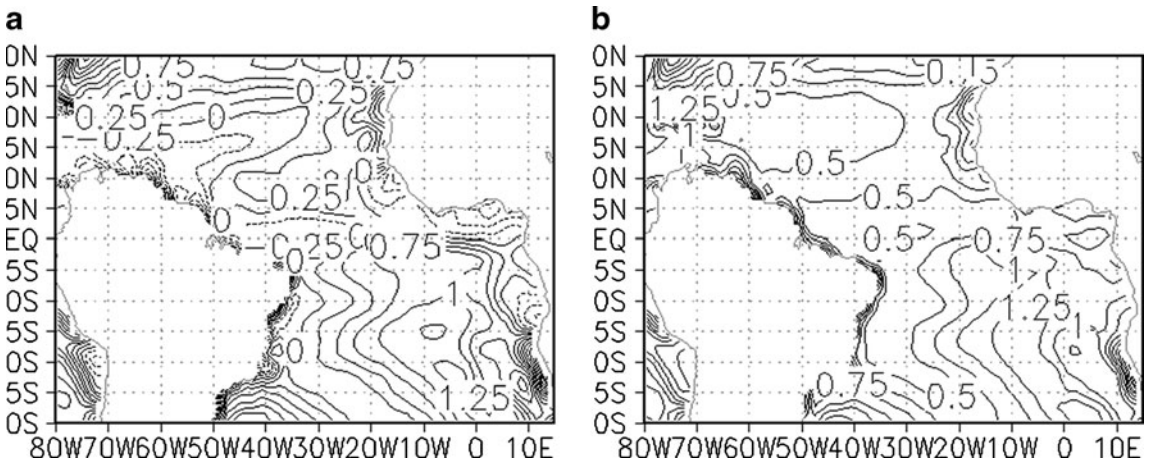

Fig. 2 SST ME (**a**) and RMSE (**b**) from CGCM, DJF mean between 1997 and 2006. Unit is degree Celsius

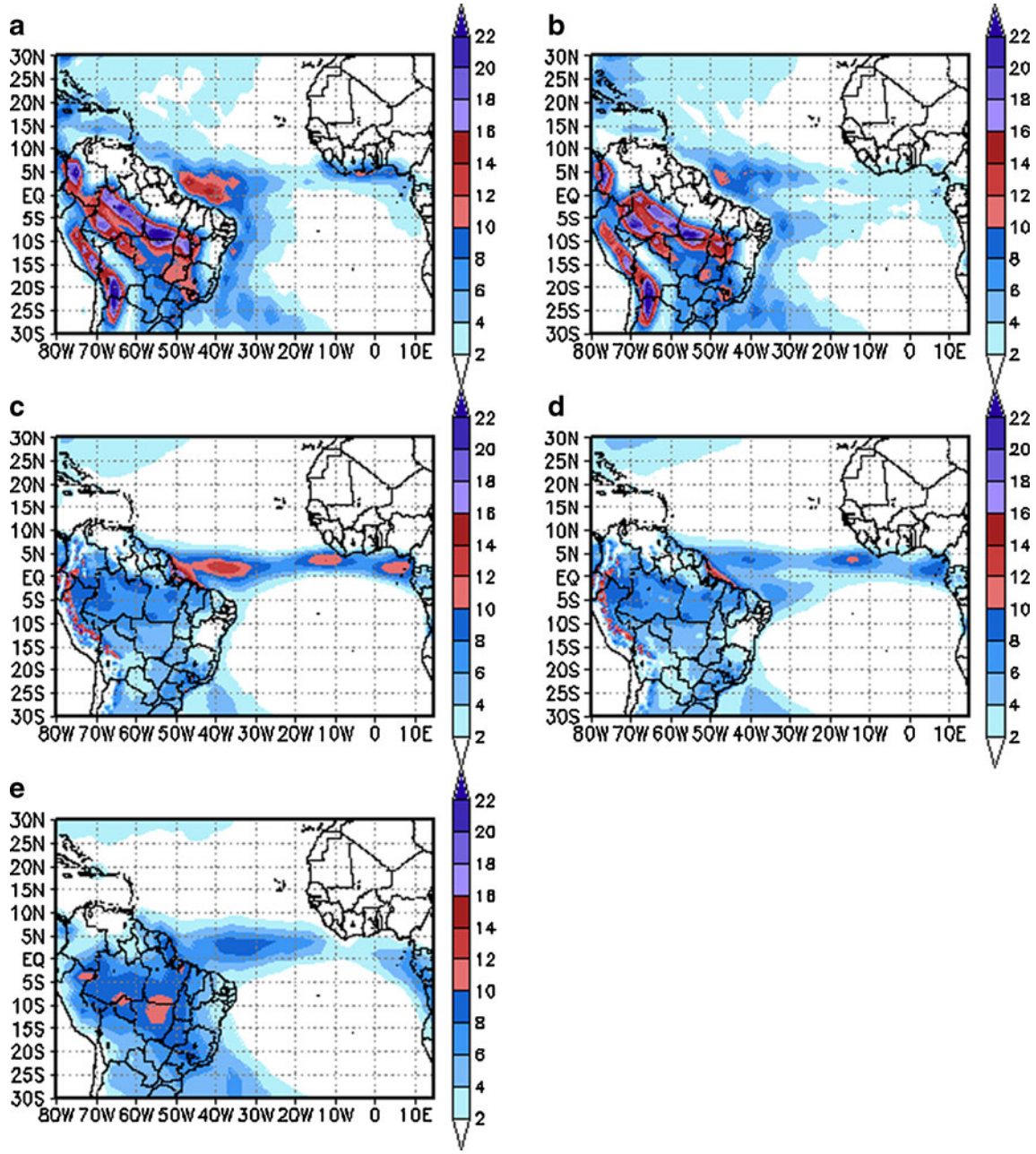

Fig. 3 Precipitation (mm day^{-1}) from (**a**) AGCM, (**b**) CGCM, (**c**) Eta + A, (**d**) Eta + C, and (**e**) CMAP, DJF mean between 1997 and 2006

made available by the National Oceanic and Atmospheric Administration (NOAA; Reynolds et al. 2002). The ocean model initialization was conducted through a forced run starting from rest and Levitus salinity and temperature global fields (NODC_WOA98 data provided by the NOAA/OAR/ESRL PSD, Boulder, Colorado, USA, from their Web site at http://www.esrl.noaa.gov/psd/), forced by NCEP reanalysis momentum fluxes (Kalnay et al. 1996) and parameterized surface heat fluxes (Rosati and Miyakoda 1988). The atmospheric initial conditions were also taken from NCEP reanalysis.

One-way nesting was applied to downscale the global models conditions using the regional model. For consistency, the limited area model used the same SST and initial atmospheric conditions as the global models. Therefore, the Eta model carried out a total of 60 seasonal range integrations.

2.4 PIRATA buoys

Ten PIRATA buoys, positioned in the tropical Atlantic (Fig. 1), were used in the validation of the forecasts. SST, precipitation, and shortwave radiation of the period between

December 1997 and February 2007 were used. Precipitation and shortwave radiation are measured at 3.5 m above sea level and the SST is measured at 1 m below sea level. Data were accessed from the address: http://www.pmel.noaa.gov/tao/disdel/disdel.html.

The value of the model grid-box, which contains a PIRATA buoy, was compared against the point value of the observation. It is expected that the inconsistency in comparing model grid-box value against observation point value is small by assuming some spatial homogeneity of properties over the ocean, and therefore observations can be representative of a large area.

3 Results

Evaluation is initially performed in terms of spatial distribution of the errors and is followed by buoy point value error evaluation. A four-way model output comparison is possible from the runs: CPTEC AGCM, CPTEC CGCM, Eta + A, and Eta + C. Part of model performance will depend on the quality of the SST, so evaluation of this field is shown before evaluating other variables. The mean error, ME, was calculated from the difference between seasonal mean of the observations, O_i, and the seasonal mean of each member j of the ensemble of simulations, $M_{i,j}$, as shown below:

$$\mathrm{ME} = \frac{\sum_{i=1}^{N}\sum_{j=1}^{M}\left(M_{i,j} - O_i\right)}{NM}$$

where i is the ith year. In analogy, the root mean square error (RMSE) is given as:

$$\mathrm{RMSE} = \sqrt{\frac{\sum_{i=1}^{N}\sum_{j=1}^{M}\left(M_{i,j} - O_i\right)^2}{NM}}$$

These errors were applied to spatial values and station point values.

3.1 Sea surface temperature

In the equatorial Atlantic Ocean, most coupled ocean–atmosphere models, which do not apply flux correction, exhibit SST zonal gradients along the equator opposite to the observations (Davey et al. 2002; Richter and Xie 2008). The latitudinal SST gradient within the latitude band between 5° S and 5° N, in DJF period, are correctly predicted by CPTEC CGCM, although the

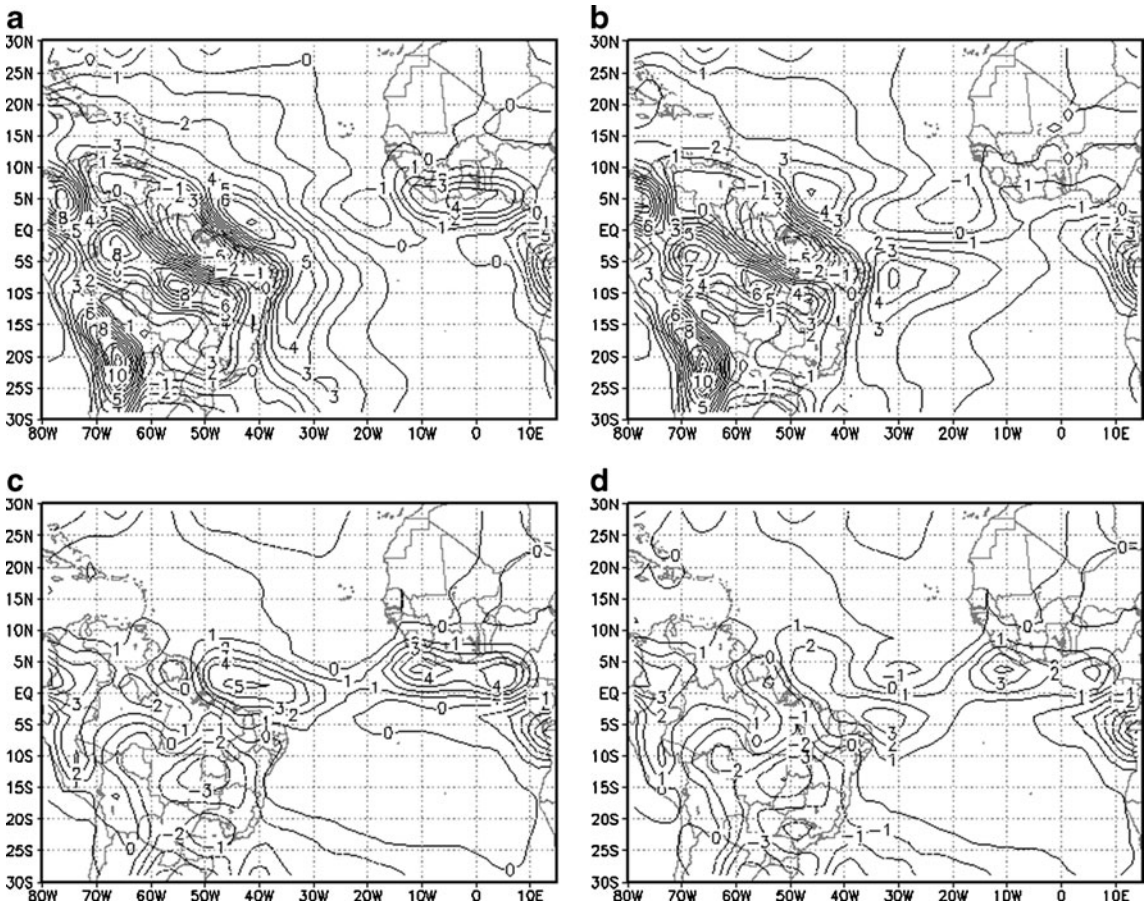

Fig. 4 Precipitation ME (mm day^{-1}) from (**a**) AGCM, (**b**) CGCM, (**c**) Eta + A, and (**d**) Eta + C, DJF mean between 1997 and 2006

minimum values are slightly displaced to the west (figure not shown). While Davey et al. (2002) carried out 20 years of continuous integrations, here 30 integrations (i.e., 3 ensemble members × 10 summers), 3.5 months forecast each were carried out. This shorter-term integrations may have contributed for improving the prediction of SST, as the coupling of the two components, atmosphere and ocean, the systematic errors of the coupled model could not reach stabilization within the short runs.

Spatial distribution of SST forecast errors are shown in Fig. 2. In most of the tropical Atlantic Ocean the SST ME is positive. Some smaller areas along the equatorial Atlantic, in southeastern Atlantic and northwestern Atlantic, negative errors were found. Huang et al. (2007) found, in general, similar error signs in the NCEP CFS system. The largest SST RMSE is found in the South Atlantic Ocean, up to about 1.5 °C, whereas the smallest errors are found in the eastern and western Atlantic Ocean.

3.2 Precipitation

The DJF mean precipitation patterns produced by the global models (Fig. 3a, b) showed similarities between each other, as the regional model driven by those conditions show more

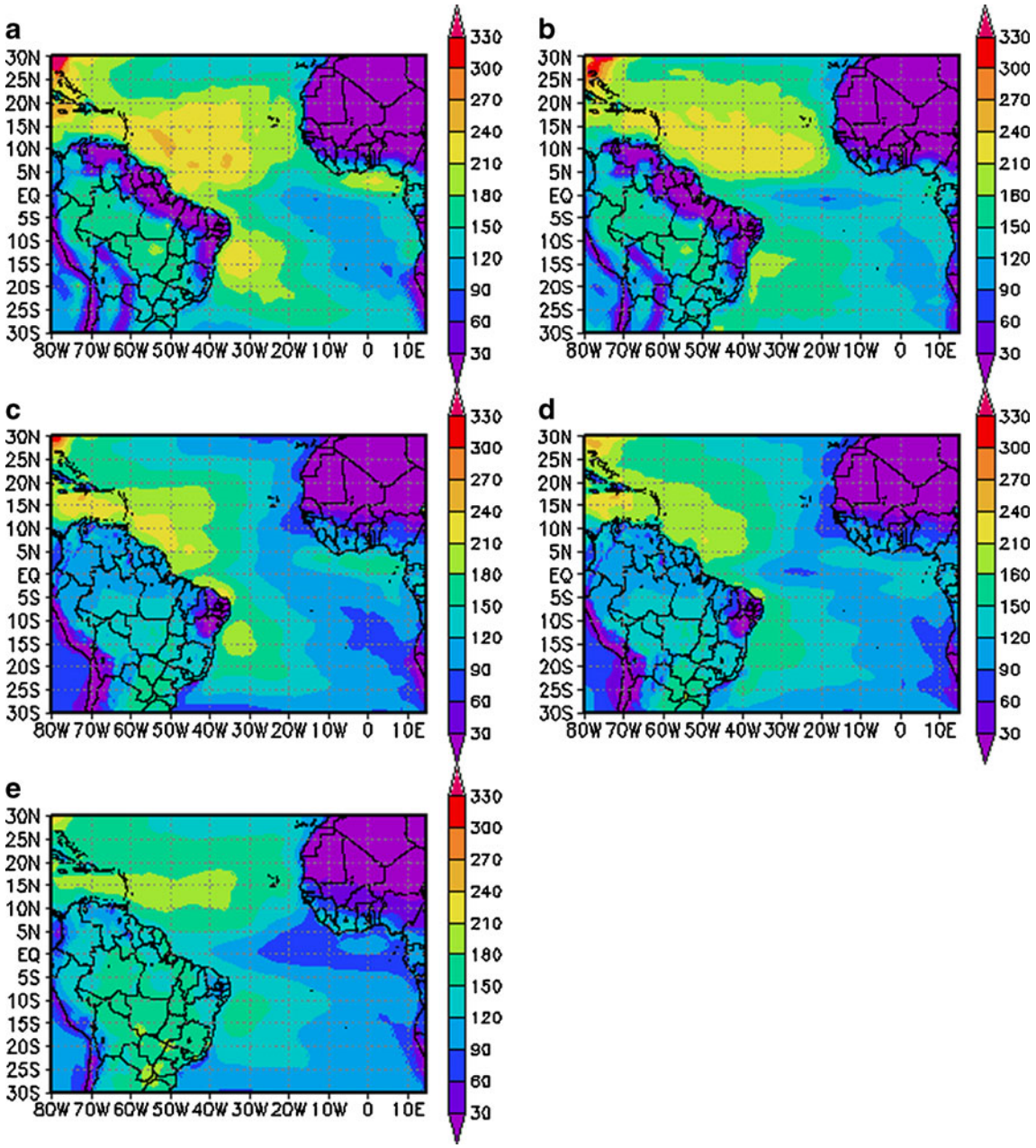

Fig. 5 Latent heat flux (W m^{-2}) from (**a**) AGCM, (**b**) CGCM, (**c**) Eta + A, (**d**) Eta + C, and (**e**) ERA-Interim, DJF mean between 1997 and 2006

similarities between each other (Fig. 3c, d) than compared with the driver model outputs. The precipitation pattern from the regional models improved considerably the precipitation forecasts over the two global models, AGCM and CGCM, according to CPC merged analysis of precipitation (CMAP) observations (Fig. 3e). This improvement occurred in most of the Eta model domain, except in the eastern Atlantic near African coast, where precipitation forecasts were worse than the driver GCMs. The cumulus convection parameterization scheme of the Eta model, although it is a simple adjustment type of scheme, has important contribution to the improvement of precipitation forecasts (e.g., Seluchi and Chou 2000). On the other hand, the GCMs which apply the RAS scheme, produce large precipitation errors over South America and tropical Atlantic (e.g., Pezzi and Cavalcanti 2000; Silva 2009).

In the western equatorial Atlantic, in the region of the ITCZ activity, the AGCM and the Eta + A produced more precipitation than the CMAP observations. This excessive precipitation may be caused by the excessive latent heat flux over the oceans in the CPTEC AGCM (Cavalcanti et al. 2002). The CGCM and the Eta + C do not show as much overestimate as the other two model outputs. This shows an advantage of the interactions of the surface fluxes over the ocean, which occurs in the CGCMs. However, the CGCM and the Eta + C show a split in the ITCZ precipitation band, which is not observed in the CMAP data. This error in the CGCM and Eta + C is probably associated with the cold SST bias produced by CGCM in this area where the split occurs (see Fig. 2a). Therefore, it is suggested that this cold SST bias may have contributed to the "double ITCZ" like band present in the CGCM and the Eta + C.

Misra et al. (2003) nested the Regional Spectral Model (Juang and Kanamitsu 1994) at 80-km resolution in the AGCM of the Center for Ocean–Land–Atmosphere Studies version 2.2 at T42L18 resolution and produced five-member simulations of January–February–March for 3 years, 1997–1999 forced by observed SST (Reynolds and Smith 1994). Their AGCM simulations of precipitation showed some similarity with the current work, however, their simulations suggest a split in the Atlantic ITCZ precipitation band, which was not found in our AGCM runs but in our CGCM runs. The RSM simulations followed closely the AGCM precipitation pattern.

Over the eastern equatorial Atlantic Ocean, the nested regional models, Eta + A and Eta + C, produced too much rain associated to the ITCZ, which is not seen in both driver global models or in the observations. It is interesting to note that Misra et al. (2003) also found this excessive rain in this region in their regional model simulations although the RSM model used in that study has different dynamics and

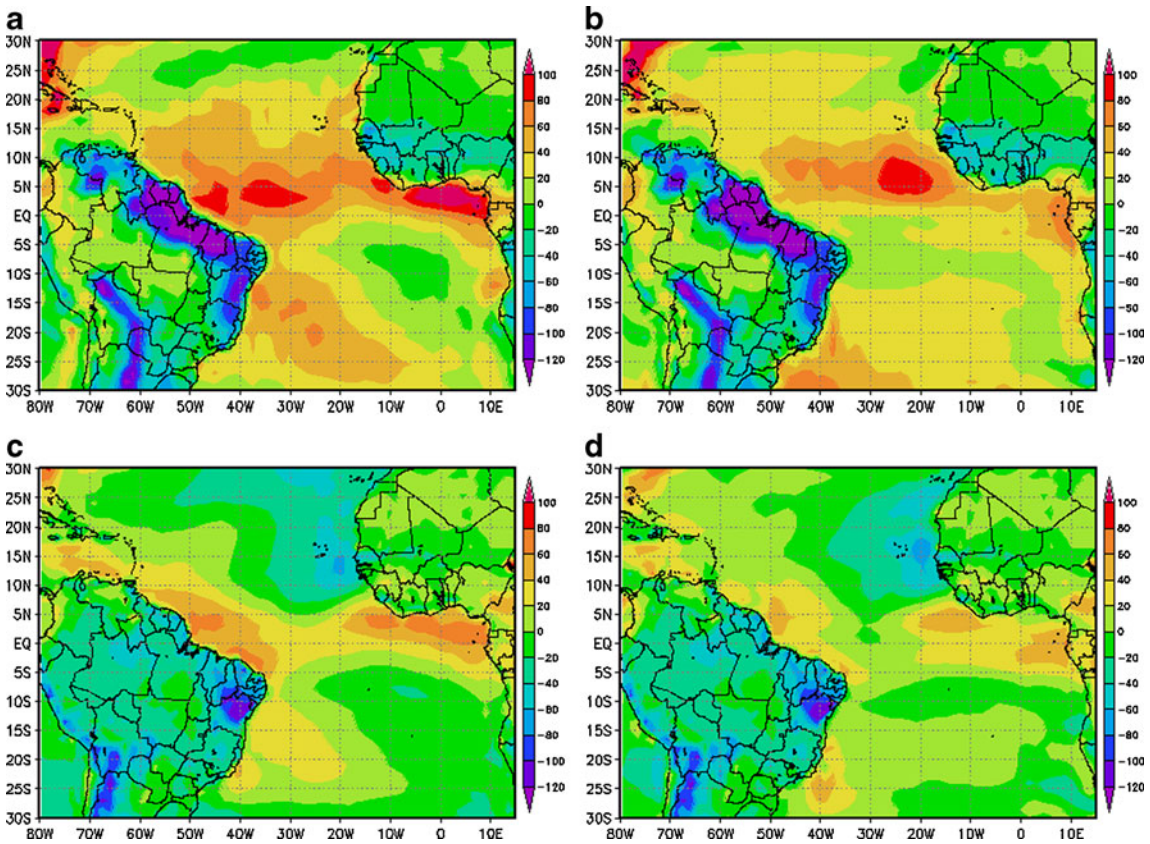

Fig. 6 Latent heat flux ME (W m^{-2}) from (**a**) AGCM, (**b**) CGCM, (**c**) Eta + A, and (**d**) Eta + C, DJF mean between 1997 and 2006

physics scheme compared to the Eta model. This error does not seem to be related to the cumulus parameterization scheme, since in Misra et al. (2003) both regional and the driver global models used RAS cumulus scheme and the excessive rain was not present in the AGCM simulations. In this region, the CPTEC CGCM produces less precipitation and cold SST bias. Over the ITCZ region, in general the Eta nested in both AGCM and CGCM global model outputs shows narrower and latitudinally elongated pattern, which resembles the observational pattern.

Along the eastern coast of Brazil, the global models produce precipitation of convective origin, which is not shown in observations (Fig. 3). The nested Eta model improves the precipitation forecasts in that area by not producing rain, but on the other hand produces excessive low clouds, as seen in Fig. 9. In Misra et al. (2003), the AGCM also produced the spurious convective precipitation in the eastern coast of Brazil. This error may be related to the RAS convection scheme used in the AGCM and RSM in Misra et al. (2003) work, since this error was not found in Cavalcanti et al. (2002) using Kuo scheme.

In the northwestern Atlantic Ocean, near the coast of South America, the global models tend to produce excessive precipitation. The two nested Eta model runs

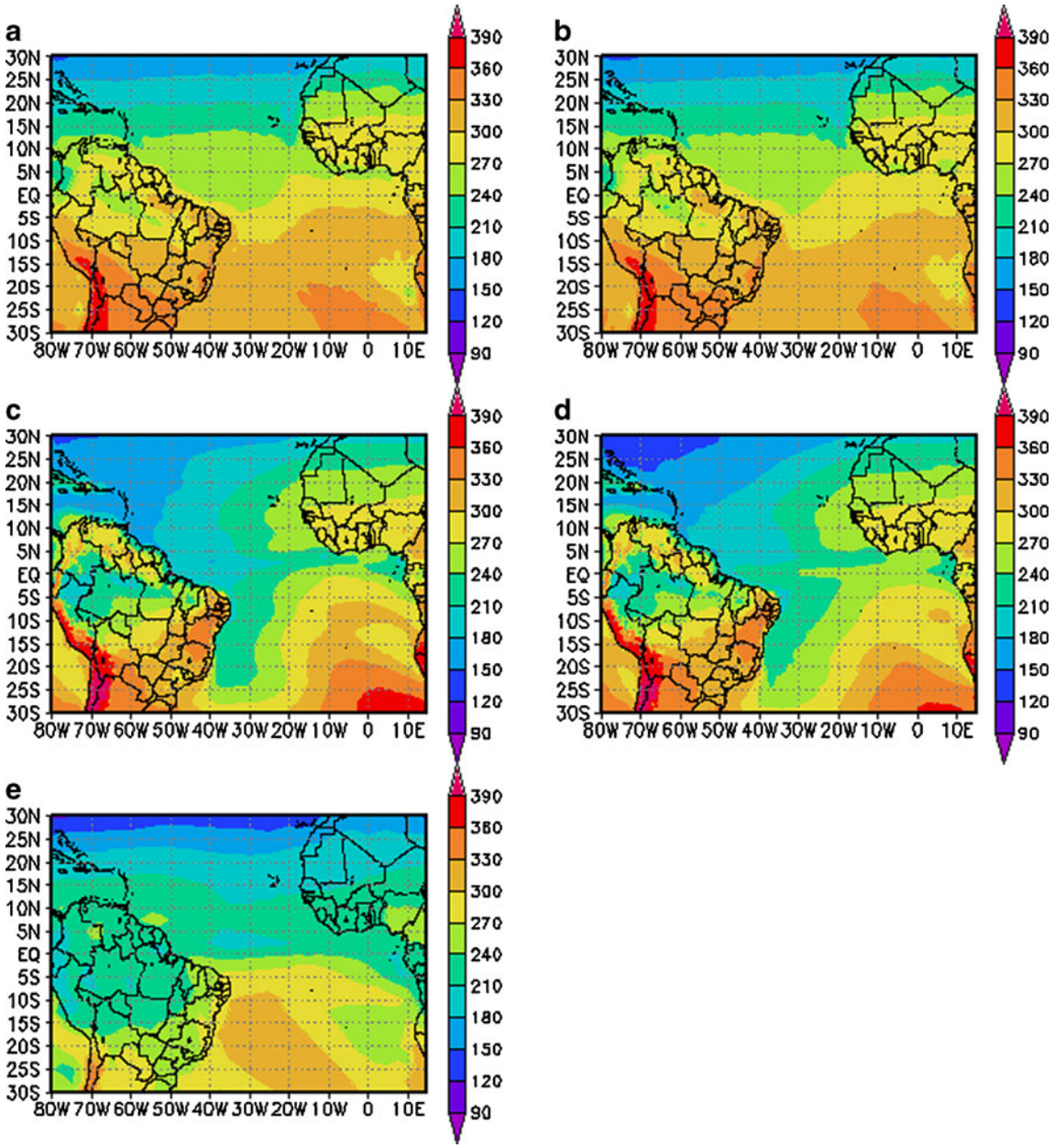

Fig. 7 Shortwave radiation (W m^{-2}) from (**a**) AGCM, (**b**) CGCM, (**c**) Eta + A, (**d**) Eta + C, and (**e**) ISCCP, DJF mean between 1997 and 2003

show smaller amounts and closer to the observations, as seen in Fig. 3.

The South Atlantic Convergence Zone (SACZ), which is a typical feature of South American summer season, is shown by the predicted precipitation band. This band extends from the Amazon toward the southwestern Atlantic Ocean. Over the continent, the CGCM had less precipitation in the SACZ than the AGCM and approached the CMAP observations (Fig. 3). The Eta + A and Eta + C improved substantially the SACZ precipitation band over the global models. This improvement was also reported by Misra et al. (2003). Over the Andes Cordillera, between southern Bolivia and northern Argentina, the global models also overestimate precipitation, which is reduced by the Eta model (Fig. 3). The spectral and coarse representation of topography may have contributed to this error in the global models as were also shown in Misra et al. (2003) and Cavalcanti et al. (2002). The CGCM has generally smaller amounts of precipitation than the AGCM, and each nested Eta run follows this feature similarly. Along the northern coast of the South American continent, the global models exhibit a wide no-rain band, which extends from eastern Colombia up to northeast of Brazil. Misra et al. (2003) and Pezzi and Cavalcanti (2000) found this same error pattern using RAS scheme. This error may be a consequence of induced subsidence from the excessive convective activity in the western Amazon and central part of Brazil. The Eta model produces less rain in the western Amazon and central Brazil, therefore the convective activity is weaker, and consequently the convection induced subsidence is also weaker. The CPTEC AGCM underestimated precipitation in the Amazon region using Kuo scheme (Cavalcanti et al. 2002) whereas it overestimated using RAS scheme in this work.

In this four-way model output comparison, the largest precipitation errors (Fig. 4), average over the 30-DJF integrations, are found in the CPTEC AGCM. Over the ocean these precipitation errors occur in the western Atlantic, near the northern and eastern coast of South America, with maximum values about 5 and 6 mm per day. The CGCM errors are generally smaller then the AGCM's, ranging about 3 and 4 mm per day over the western Atlantic and extending farther eastward. The Eta model nested in these two global models has considerably reduced the precipitation errors over the continent and over the ocean, with Eta + C exhibiting the smallest error among the four models precipitation outputs.

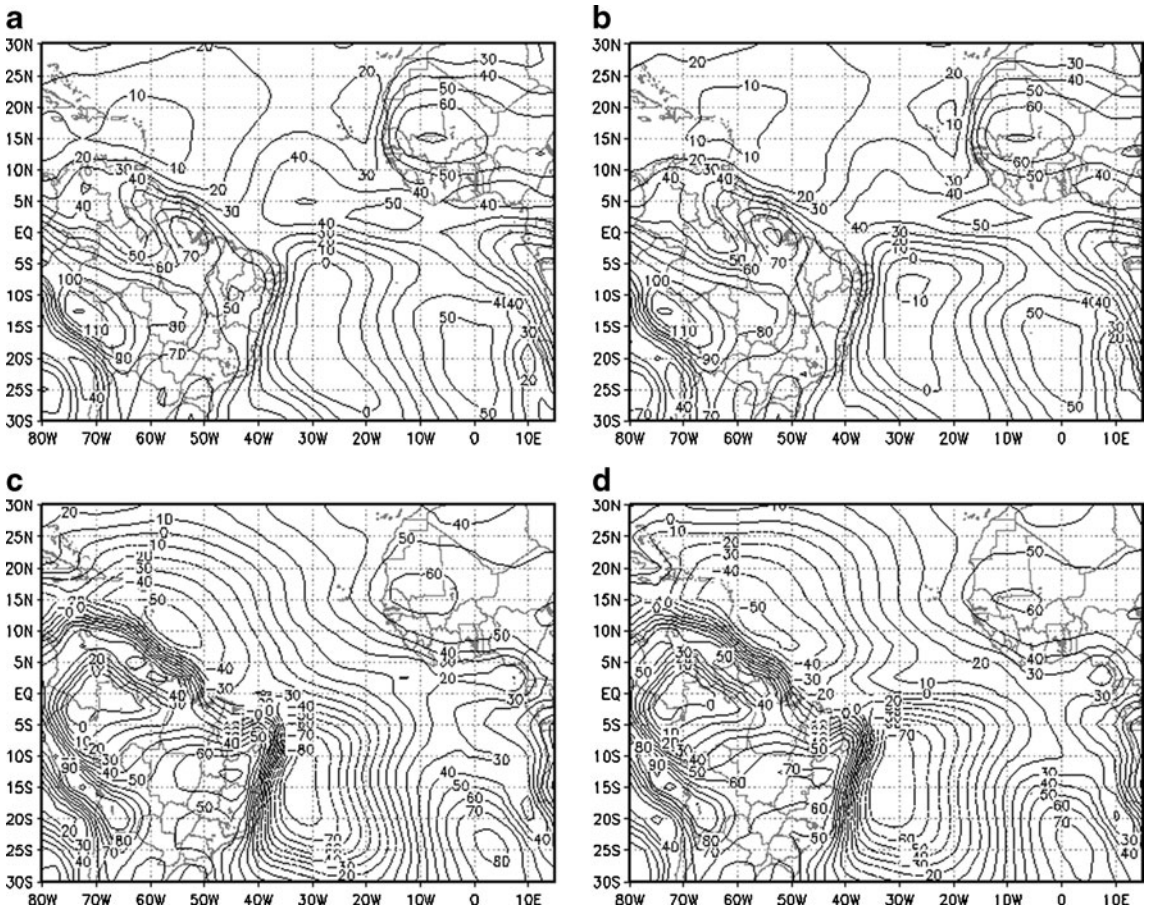

Fig. 8 Shortwave radiation ME (W m^{-2}) from (**a**) AGCM, (**b**) CGCM, (**c**) Eta + A, and (**d**) Eta + C, DJF mean between 1997 and 2003

3.3 Latent heat flux

Over the tropical regions domain, the latent heat flux fields show similar spatial patterns in both global models (Fig. 5a, b). The latent heat flux fields of the nested Eta runs are also similar to each other (Fig. 5c, d), despite the quite distinct patterns produced by the global models they are nested in. This suggests the strong control of the atmospheric component on the surface latent heat flux. Both global models share the same atmospheric component (i.e., the AGCM), which is different in many aspects, dynamics and physics, from the regional model. The global models use different schemes from the regional model to treat surface fluxes, over land and over the ocean (see Sections 2.1 and 2.2).

All models reproduce the two centers of maxima in both hemispheres of latent heat flux, which results from the strong northeasterly and southeasterly trade winds that blow in the equatorial region. The nested Eta model outputs show latent heat flux fields closer to reanalysis (Fig. 5e), in particular the Eta + C, in comparison with the driver global models. The latent heat flux is partially affected by the driver model through the lateral boundary conditions. The AGCM exhibits higher latent heat flux than the CGCM by about 30 W m^{-2}, and the nested Eta + A also exhibits higher latent heat flux than the Eta + C by similar amount (Fig. 5). This excess of latent heat flux is caused by the prescribed SST in the AGCM, which therefore lacks the negative feedback processes of surface temperature cooling, inherent in the CGCM one-tier simulations. The latent heat flux reproduced by CPTEC CGCM is similar to the values obtained by Huang et al. (2007) in the Northern Hemisphere, but higher in the Southern Hemisphere. In the Gulf of Guinea, the CGCM also exhibits similar values to those of Huang et al. (2007), but the CPTEC AGCM strongly overestimates the flux, by about 90 W m^{-2} in comparison with reanalysis values. This error was partly transmitted to the Eta + A.

In the southeastern tropical Atlantic Ocean, the latent heat flux from CGCM is higher than the AGCM (Fig. 5b). This error coincides with the area of warm SST bias of the CGCM, and is reproduced by the regional model. The Eta + C exhibits higher flux than the Eta + A in that region. In the southern Atlantic Ocean, the AGCM tops the overestimation of the latent heat flux, followed by the CGCM. The Eta + C exhibits the smallest errors in the region. In the northern part of South America and northeast of Brazil regions, the latent heat flux reproduced by the global models are smaller than reanalysis, Eta + A and Eta + C values. This error may be partly caused by the lack of local moisture source, as it is the region where the global model does not produce enough precipitation.

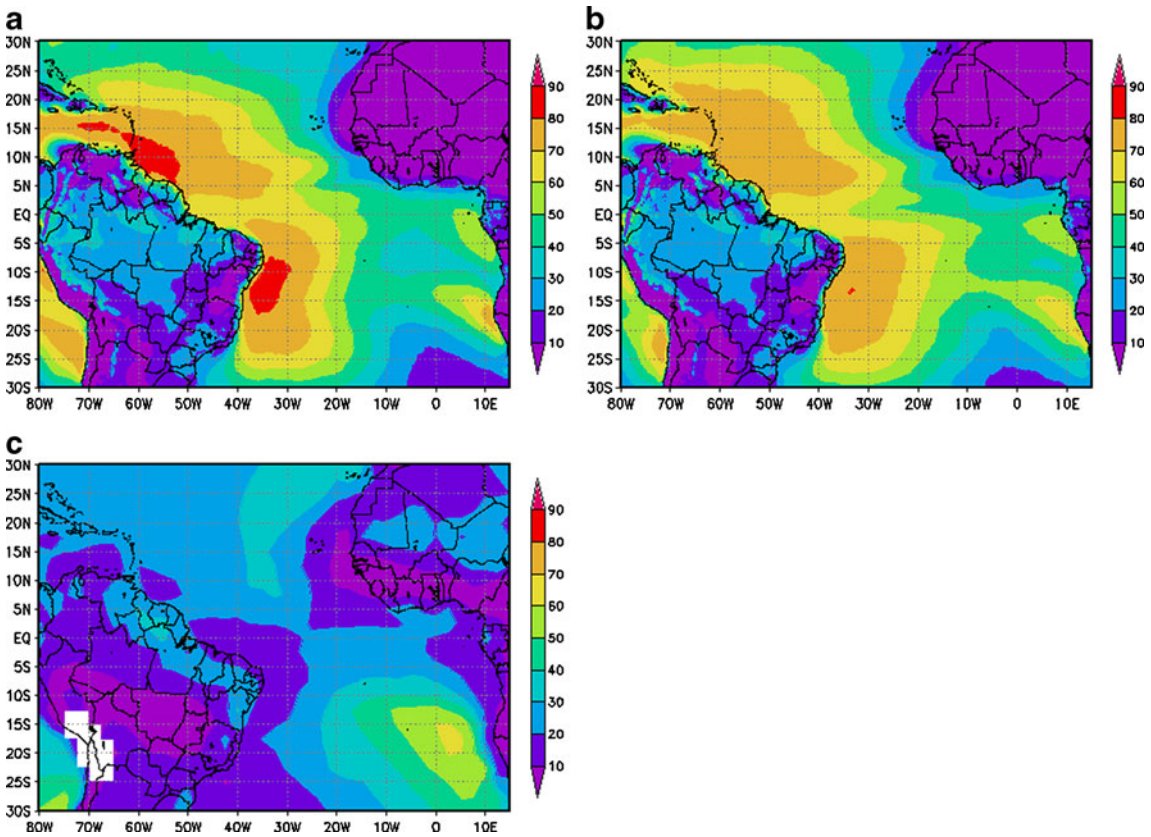

Fig. 9 Low cloud cover (%) from (**a**) Eta + A, (**b**) Eta + C, and (**c**) ISCCP, DJF mean between 1997 and 2003

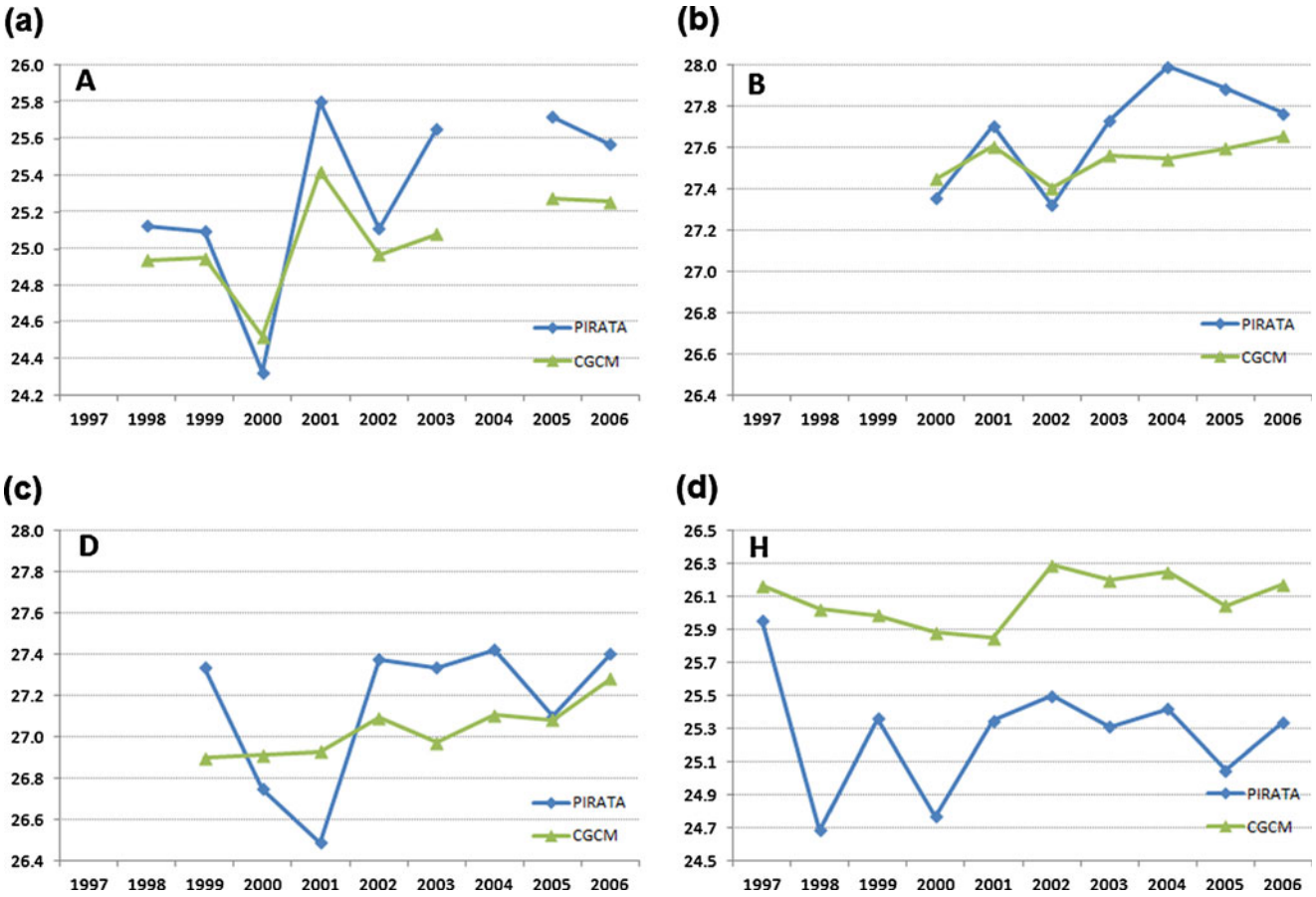

Fig. 10 Interannual variability of DJF mean SST of buoys (**a**) A, (**b**) B, (**c**) D, and (**d**) H in comparison with CGCM

The global models overestimate the latent heat flux up to 100 W m^{-2} along the latitude 5° N (Fig. 6a, b) where the mean errors from the Eta runs (Fig. 6c, d) are smaller, in particular the errors in the Eta + C are the smallest. In the northeastern part of the tropical Atlantic Ocean, the global models overestimate the fluxes by about 40 W m^{-2}, whereas the Eta runs underestimate about 60 W m^{-2}. Over the Southern Hemisphere, the errors of the nested Eta runs are smaller than the errors of the global models, reaching values up to about 40 W m^{-2} in the southwestern Atlantic.

Table 1 SST (°C) ME, RMSE, and temporal correlation (*r*) between CGCM and buoy point

Buoys	ME	RMSE	*r* value
A	−0.25	0.90	
B	−0.13	0.58	0.77
C	−0.30	0.73	
D	−0.12	0.85	0.54
E	−0.10	0.40	
F	−0.13	0.50	
G	0.03	0.36	
H	0.81	2.63	0.51
I	−0.15	0.33	
J	−0.01	0.24	

3.4 Shortwave radiation

In general, the pattern of the incoming shortwave radiation (SWR) at the surface of the AGCM (Fig. 7a) is similar to the pattern of the CGCM (Fig. 7b), but different from the SWR pattern produced by the Eta + A (Fig. 7c) and Eta + C (Fig. 7d). The CPTEC global model and the Eta model employ the same SWR scheme, which would suggest the similar error pattern between global and regional models. However, a closer look shows that the low cloud coverage is different for both models. The global models have simple stratiform cloud, whereas the regional model has complex cloud microphysics scheme. The different spatial distribution of low clouds affected the surface incoming SWR.

In the region between the ITCZ and 30° S, both Eta + A and Eta + C underestimate the SWR in comparison with the International Satellite Cloud Climatology Project (ISCCP) observations (Fig. 8). Note that mean values are calculated in a shorter period (1997–2003), when ISCCP data are available. Figure 9

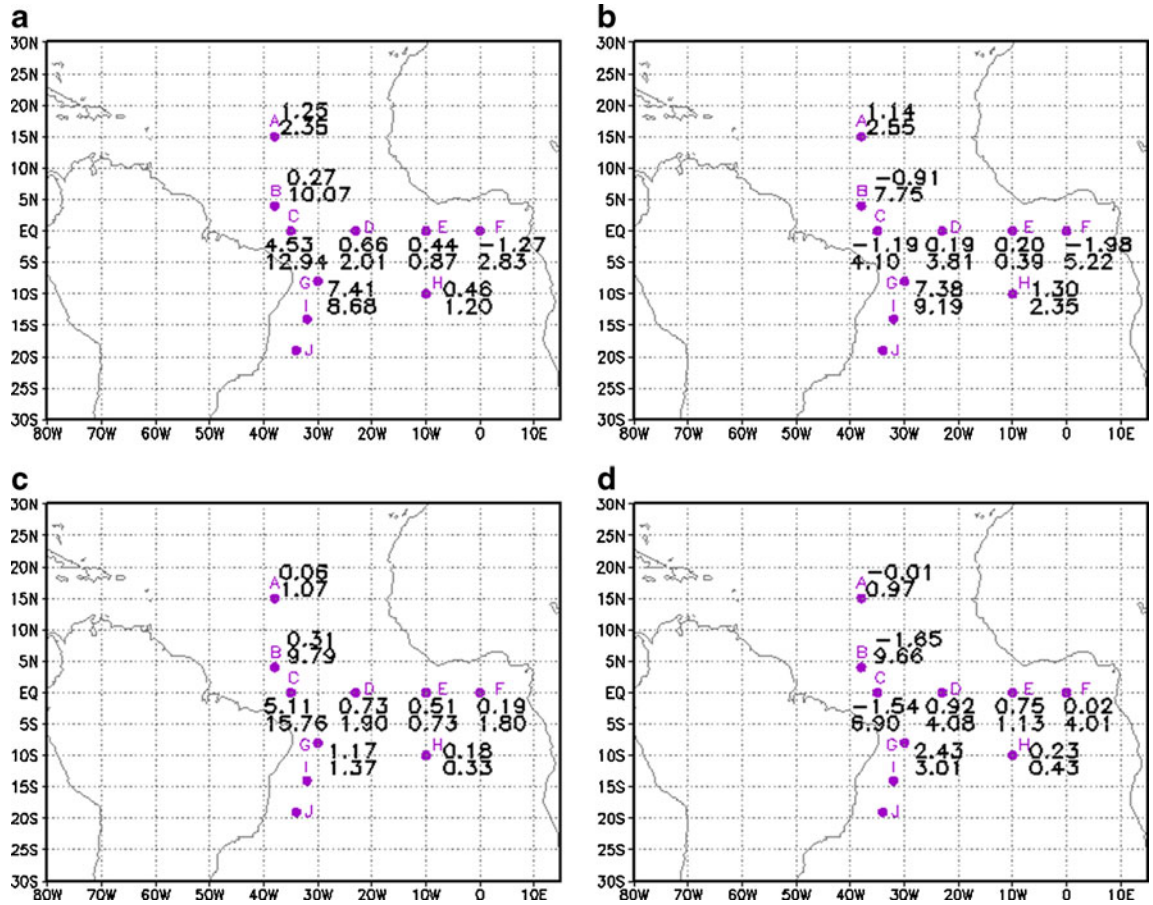

Fig. 11 Precipitation (mm day^{-1}) ME (*number above*) and RMSE (*number below*) from (**a**) AGCM, (**b**) CGCM, (**c**) Eta + A, and (**d**) Eta + C, at each PIRATA buoy position

shows the pattern of low cloud cover of the nested runs. Note that SWR errors occur over the same region where the Eta model overestimates the low cloud coverage (Fig. 9), suggesting the blocking of the downward SWR before reaching the surface. The global models had excessive convective precipitation in that region. However, the associated optical depth does not seem efficient enough to block the downward SWR as the surface SWR from the global models is higher than Eta runs and closer to the observations. In the Guinea Gulf region, the SWR from the Eta + A and Eta + C is closer to the observations than the global models. In the southeastern Atlantic Ocean, all models produce large errors; the regional model overestimates the SWR there, where it produces few low clouds. Over the continent, all models generally show large errors, except over the western Amazon where the Eta + A and Eta + C exhibit values close to the observations (Fig. 7).

Table 2 Precipitation and SWR ME, RMSE, average in all buoys, from AGCM, CGCM, Eta + A and Eta + C

Average		AGCM	CGCM	Eta + A	Eta + C
Precipitation (mm day^{-1})	ME	1.72	0.77	1.03	0.14
	RMSE	5.12	4.42	4.09	3.77
SWR (W m^{-2})	ME	34.35	34.76	−19.64	−13.41
	RMSE	85.41	83.56	78.53	65.42

Over the western basin of the South Atlantic Ocean, the global models exhibit the smallest mean errors of incoming surface SWR (Fig. 8a,b) whereas the Eta + A and Eta + C (Fig. 8c, d) exhibit strong negative bias, of about −80 W m^{-2} by Eta + A, and about −70 W m^{-2} by Eta + C. In the Guinea Gulf region, the global models mean errors are positive and larger than the nested regional model errors. Over the southeastern Atlantic Ocean, all models overestimate the SWR, in particular Eta + A. According to Carton et al. (2005), this excessive SWR in that region of South Atlantic is due to the deficit in the models of low cloud cover, which maintains the warm SST bias frequently found in coupled ocean–atmosphere global models. On the other hand, Hu et al. (2011) replaced the model global low clouds by ISCCP monthly low clouds (LCA2 exp.), and they found that the improved low cloud cover only had a minor influence on the amount of net shortwave radiation reaching the surface (see their Fig. 3) in the southeastern Atlantic in the NCEP CFS model. They suggested that low cloud cover plays

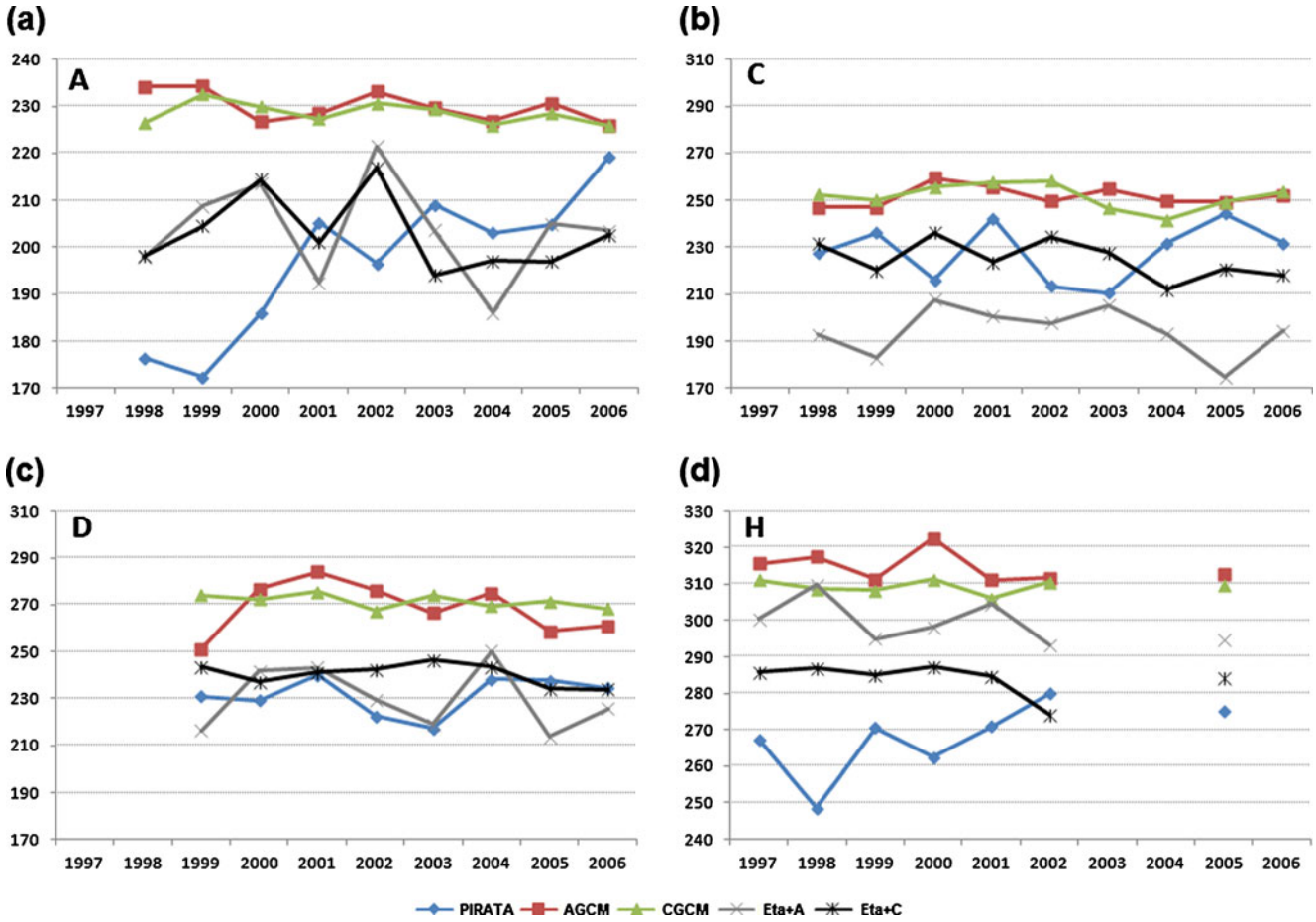

Fig. 12 Interannual variability of DJF mean shortwave radiation (W m^{-2}) of buoys (**a**) A, (**b**) C, (**c**) D, and (**d**) H in comparison with AGCM, CGCM, and nested Eta runs

a secondary role in blocking and absorbing the radiation in the radiation parameterization scheme of the model. Over the continent, the Eta + A and Eta + C mean radiation errors are positive, but still smaller than the global models mean errors.

Evaluation of model Outgoing Longwave Radiation (OLR) was carried out in comparison with ISCCP data (Figures not shown) and showed that all models overestimated OLR, but the Eta + C only marginally produced smaller errors than the other runs.

3.5 PIRATA buoy validation

The SST, precipitation, and SWR produced by the models are compared against the ten time series measured by the PIRATA buoys distributed over the Atlantic Ocean, as shown in Fig. 1. Buoys are identified by the letters A to J, and are distributed in various regions over the tropical Atlantic. Linear correlations between seasonal mean of the observations and of the three-member mean of the SST simulation were calculated in order to evaluate model capability to capture interannual variability.

3.5.1 Sea surface temperature

The interannual variability of SST is well captured by the CGCM in the buoys A, B, and H (Fig. 10a, b, d). Yet, in buoy H, in the central part of the South Atlantic basin, the SST variability from CGCM is smaller than the buoy, and the CGCM does not show the peaks in 1998 and 2000. Also, the model fails to capture the interannual variability in the buoys C (figure not shown) and D (Fig. 10c), which are located along the equator. Yet, the model seems to capture the linear temporal trend of the summers of the period. Due to data gaps in the time series in buoys E, F, G, I, and J, the interannual variability cannot be evaluated there.

In terms of ME, the CGCM underestimates the SST measured in most of the buoys, except in G and J, located in the western basin of the South Atlantic Ocean, where errors are negligible, and in buoy H where errors are large and positive (Table 1). This warm SST bias is a common error produced by the coupled ocean–atmosphere global models around this region. The RMSE of SST in H is just

over 1 °C. The mean errors calculated with respect to these PIRATA buoys, averaged over the ten summer seasons, are similar to errors with respect to the NOAA OI SST (see Fig. 2a). Correlation between the times series are possible for buoys B, D, and H where observations series were continuous in time. Correlations were all higher than 0.5, in particular in buoy B, northern Atlantic, where correlation reached 0.77, which shows that the SST produced by the CGCM follows correctly the temporal variability of SST on those regions.

3.5.2 Precipitation

Due to gaps in the precipitation time series of the PIRATA buoys, the interannual variability could not be accurately evaluated. But it was noted the consistency among the buoys, for example in buoys B and C, located along the equator, are the rainiest stations, whereas buoy H, located in the middle of the South Atlantic ocean, has small amount of precipitation.

Figure 11 shows the spatial distribution of model precipitation mean errors and RMS errors from comparison against buoys measurements. In the buoy A, the nested Eta runs produce marginal errors and generally smaller than the global model errors. The buoys B and D show large ME and RMSE from all models. The magnitudes of the errors of Eta + A and Eta + C approximately follow the error magnitudes of the global models, but the nested runs generally exhibit smaller errors, which is consistent with comparison against CMAP mean data (Fig. 4).

In the buoy G area, located near the coast of northeast of Brazil, the global models have large positive ME, which is a result of spurious convective precipitation. The nested runs also have positive errors in that area, but at much smaller magnitude. The buoys I and J were not evaluated due to problems in the dataset. From the average over the eight buoy errors (Table 2), the Eta + C exhibited the smallest mean precipitation error.

3.5.3 Shortwave radiation

In comparison with the nested Eta runs, the global models show weaker interannual variability of the SWR in DJF in all the evaluated buoys: A, C, D, and H (Fig. 12). The other buoys are not evaluated due to buoy data gaps. In those evaluated

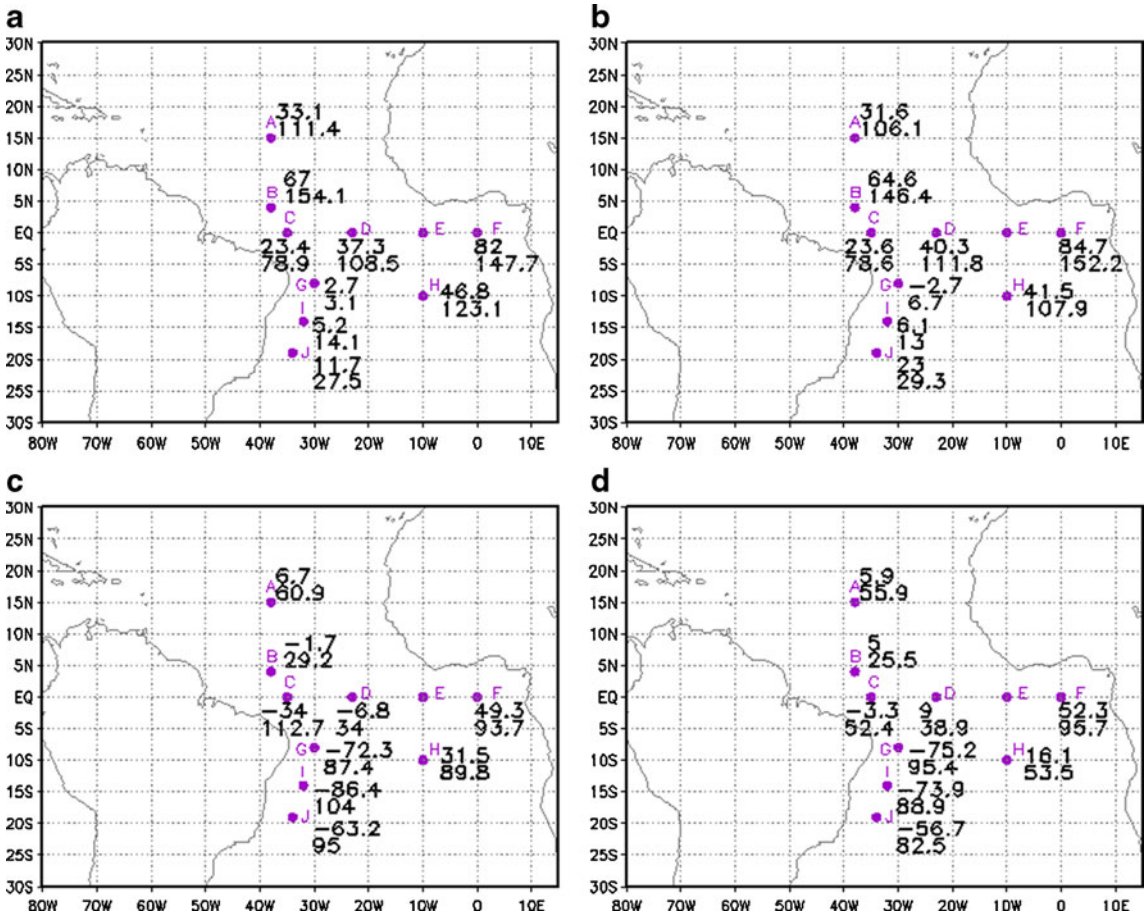

Fig. 13 Shortwave radiation (W m^{-2}) ME (*number above*) and RMSE (*number below*) from (**a**) AGCM, (**b**) CGCM, (**c**) Eta + A, and (**d**) Eta + C, at each PIRATA buoy position

points, the global models overestimate the radiation, whereas the nested model values are closer to the observations. Moreover, both CGCM and AGCM SWR values are very similar to each other, whereas both Eta + A and Eta + C exhibit large differences in their magnitudes. The observed interannual variability is hardly captured by the models, except in buoy D, where the Eta + A follows closely the buoy curve.

Figure 13 shows all model errors in SWR with respect to the buoy observations. The Eta model nested in CPTEC global models generally have smaller RMS errors than their driver models; except in the area of buoys C, G, I, and J, which are located in the South Atlantic near the coast of South America, where the Eta model largely underestimate the SWR. This negative ME is also found in comparison against ISCCP observations (Fig. 8). The global models overestimate the SWR in most of buoy points.

The Eta runs produce smaller errors than the global models in six out of nine buoy locations. Considering the ME, the Eta + C shows the smallest errors among the models (Table 2). The regions over the Atlantic near the coast of South America require attention in the regional model due to the clear systematic negative bias in SWR. In general, the Eta + C show better model performance. It should be noted, however, that the evaluation was based mostly on precipitation and SWR and a few points distributed over the Atlantic Ocean; and that various time gaps were found in the dataset. The errors found in the few buoy points do agree with the error signs found in other sources of verification data, e.g., Era-interim reanalysis and ISCCP.

3.6 Boundary forcings

The Eta + A and Eta + C have exactly the same setup. The differences in the runs lie only in the lateral boundary conditions in the atmosphere and lower boundary conditions over the ocean. In order to investigate the causes for the Eta + C general better forecasts than Eta + A, the errors of the forcings through the lower boundary conditions in term of SST and the lateral boundary conditions were assessed. Figure 14 shows the ME and RMSE of predicted SST from the CGCM and the persisted anomaly SST used in AGCM. It shows that both errors are larger in the predicted than in the persisted SST.

Figure 15 shows the RMSE of the zonal wind at 850 hPa and geopotential height at 500 hPa, which can be representative of the large-scale flow. It is speculated that large-scale forcing

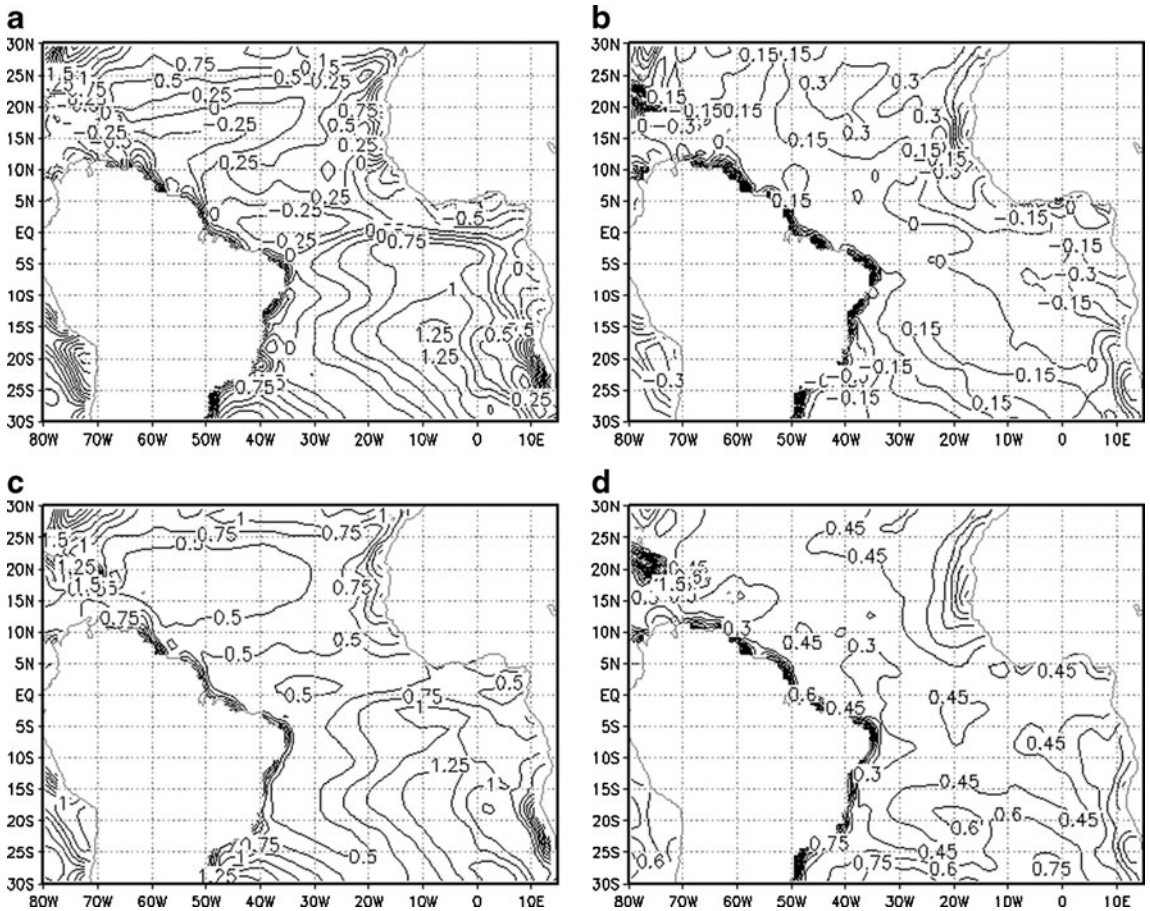

Fig. 14 Mean error (*top row*) and root mean square error (*bottom*) of predicted (**a**, **c**) and persisted anomaly (**b**, **d**) sea surface temperature. Units are degree Celsius

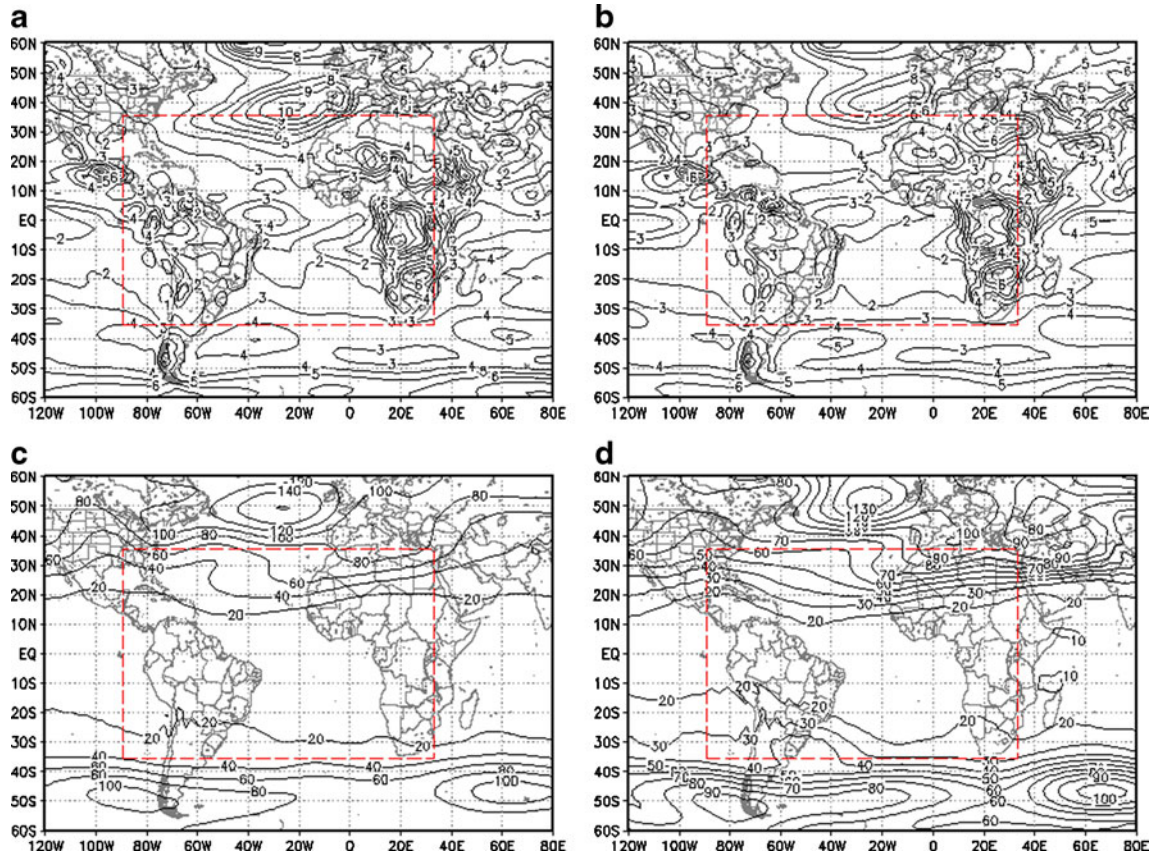

Fig. 15 Root mean square error of 850-hPa zonal wind (*top row*) and 500-hPa geopotential height (*bottom row*), from AGCM (*left*) and CGCM (*right*). The red box corresponds to the Eta model lateral boundaries. Units are meters per second and meters, respectively

provided by CGCM had smaller errors and, therefore, better quality. Figure 15 shows that the RMS errors of the wind and of the geopotential height, in particular near the lateral boundaries where large-scale information is transmitted to the regional model, exhibit larger values in the AGCM than in CGCM. The Eta model does not apply any nudging, either in the boundary conditions or internal domain. It was shown in Chou et al. (2002) that in long-term integrations, the regional model is strongly constrained by the atmospheric lateral boundaries, more than the ocean lower boundary. Therefore, although the CGCM had larger SST errors than the persisted AGCM in these runs, the former had smaller errors in the wind than the AGCM, which resulted better large-scale circulation values transferred laterally to the regional model. Therefore the improvement of the regional model runs over the GCM runs are probably due to the regional model resolution and physics, while the better performance of the Eta + C over Eta + A is probably due to the better large-scale forcing description of the CGCM over AGCM.

3.7 Ensemble spread

In order to verify whether the ensemble members envelop the observations, the spread of the members is compared against the RMSE. It is expected that spread and RMSE have similar magnitudes. Standard deviation of the members of the 10-year mean of the seasonal precipitation was calculated at each grid-point. The global and regional models precipitation was interpolated to the CMAP grid (2.5° latitude×2.5° longitude). Figure 16 shows the scatter plot between the standard deviation and RMSE of DJF precipitation. The plot distinguishes the grid points over the continent from the ocean. All points of all models exhibit RMSE much larger than the ensemble spread as all grid points lie below the solid line. The figure also shows that the global models have large precipitation errors over the continent. Both Eta versions have smaller error over continent, but on the other hand the spread is slightly smaller than the global models. Over the ocean, scatter plot of the global models are similar to the regional models.

The magnitude of the spread of other variables, such as latent heat flux, shortwave radiation, 1000-hPa temperature, and 850-hPa geopotential show values much smaller than the respective RMSE (figures not shown), both in the global and regional models. One could argue that the small spread with respect to the RMSE is due to the small number of members of the ensemble. A ten-member ensemble of the AGCM and CGCM was tested for the DJF 2005/2006 season and compared against the three-member ensemble of the same season

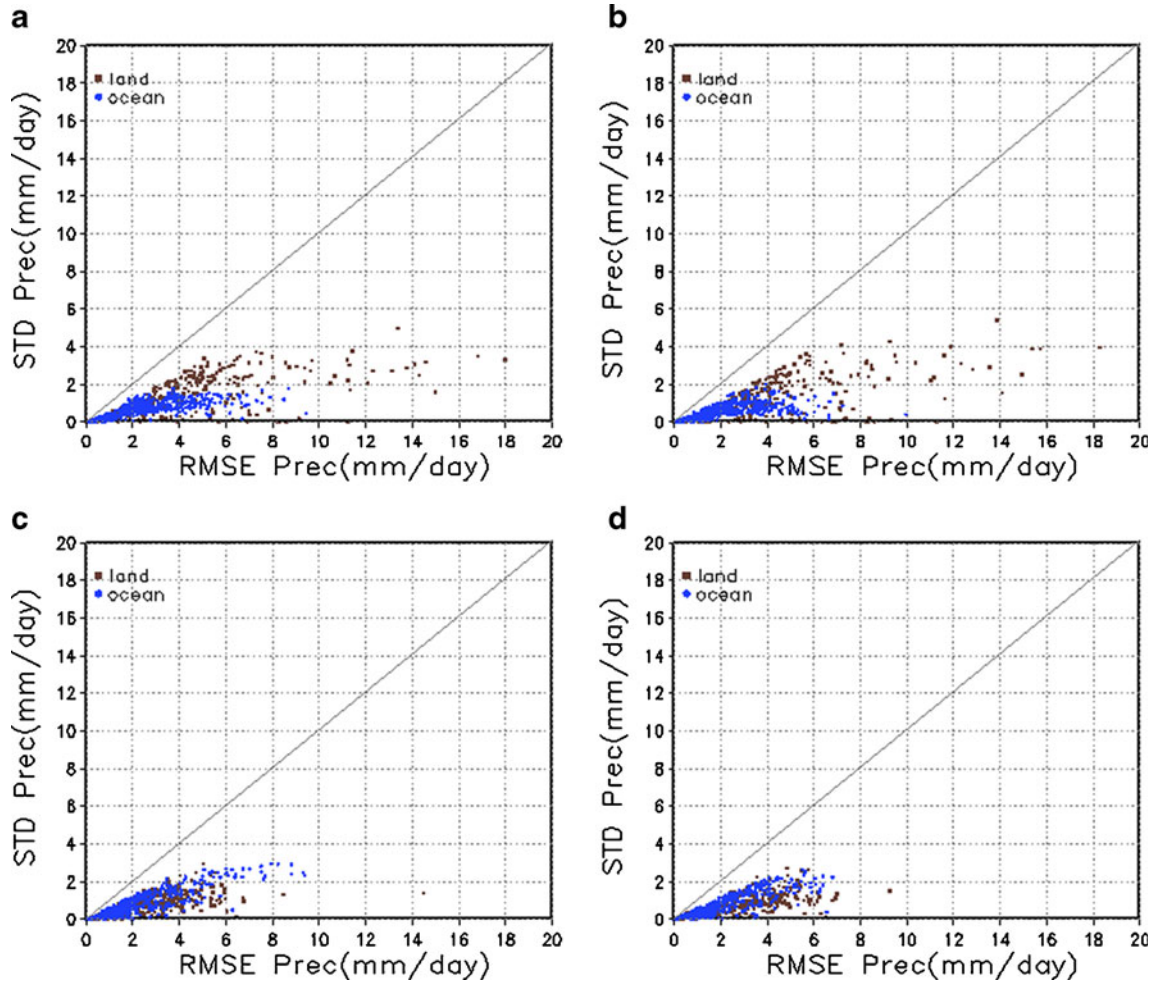

Fig. 16 Scatter plot between the RMSE and the standard deviation of DJF precipitation (mm day^{-1}) mean over 1997–2006 for the ensemble members of (**a**) AGCM, (**b**) CGCM, (**c**) Eta + A, and (**d**) Eta + C, of *all grid points*. The *blue points* correspond to grid points over the ocean, while the *brown points* refer to grid points over the continent

(Fig. 17). The increase in the number of members resulted in no evident increase in the ensemble spread.

This assessment shows that the model errors are too large and that they should be reduced before increasing the number of the ensemble members.

4 Conclusions

Hindcasts of 10 years of austral summer season for the months of DJF are generated by the CPTEC atmospheric and coupled ocean–atmosphere global general circulation models using persisted and forecasted SST anomalies, respectively. The Eta model is nested in these runs at 40-km resolution over the domain that encompasses the tropical Atlantic Ocean, and parts of South America and western Africa. The results shown so far demonstrate the added value of the dynamical downscaling using the Eta regional atmospheric model of these two global model conditions. The evaluation considers the average of three members of 10 years, between 1997 and 2006, of 3.5-month integrations for the austral summer season, DJF.

Evaluation of the hindcasts of SST from CPTEC CGCM showed correct latitudinal gradient near the equatorial Atlantic and errors of magnitude of about 0.5 °C, which can be considered small. Over the southeastern Atlantic, which is a region where the CGCMs commonly produce large SST warm bias, the CPTEC CGCM generated a mean error of up to 1.25 °C.

The nested Eta model improves the precipitation forecasts over the AGCM and the CGCM, in comparison with CMAP observations. This improvement occurred in most of the domain, except in the eastern Atlantic near African coast. Although, the CGCM produced a split in the ITCZ precipitation band, the CGCM produced the smallest precipitation errors in comparison with AGCM. The Eta model nested in the CGCM showed the best results for precipitation.

The nested Eta model runs improved the latent heat flux hindcasts, in particular the Eta + C, in comparison

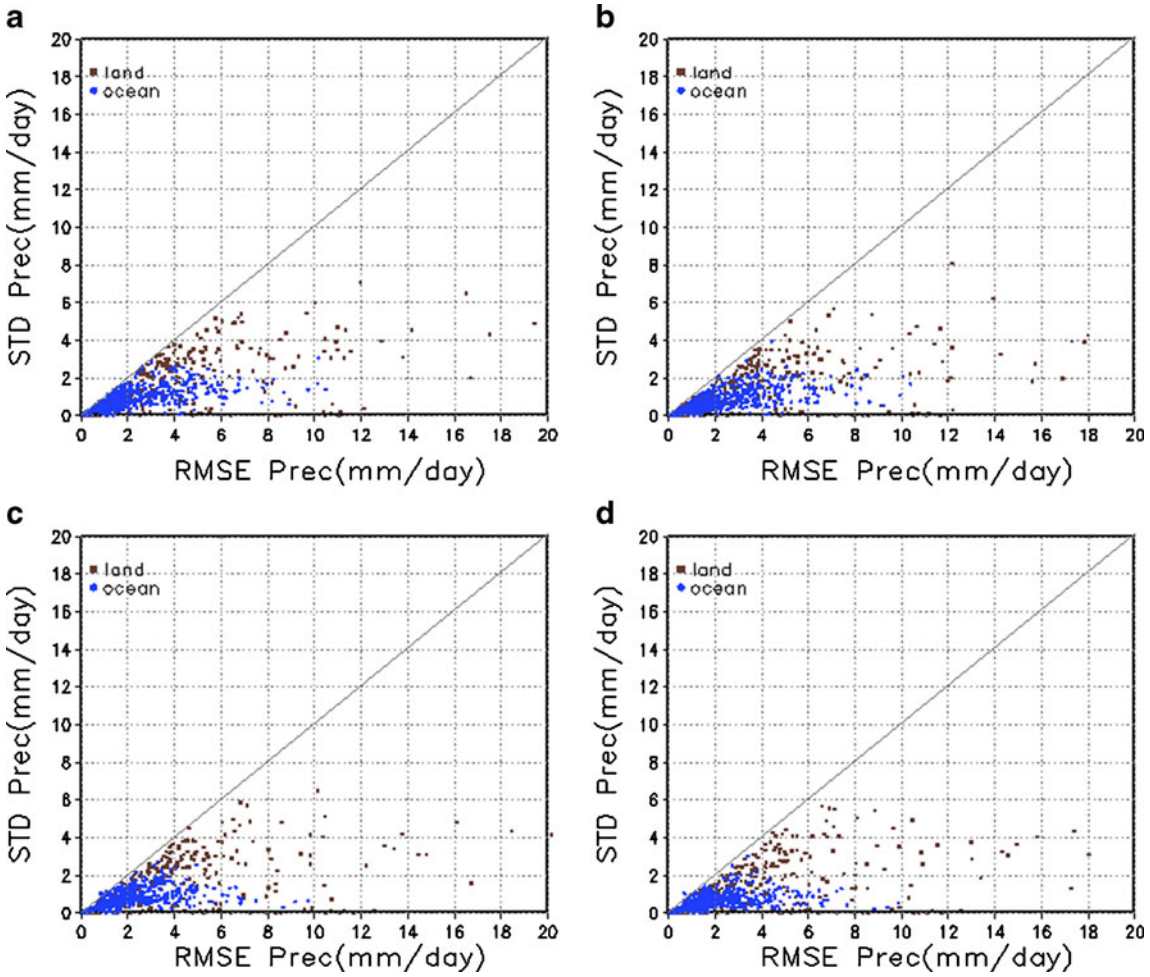

Fig. 17 Scatter plot between the RMSE and the standard deviation of 2005–2006 DJF precipitation (mm day^{-1}) for the ensemble of (**a**) AGCM with ten members, (**b**) AGCM with three members, (**c**) CGCM with ten members, and (**d**) CGCM with three members, for *all grid points*. The *blue points* correspond to grid points over the ocean, while the *brown points* refer to grid points over the continent

with the driver global models. Over the ocean, the AGCM overestimated the latent heat flux more than the CGCM. This excess of latent heat flux is caused by the prescribed SST in the AGCM, which therefore lacks the negative feedback processes of surface temperature cooling, inherent in the CGCM one-tier simulations. Except over the southeastern Atlantic Ocean, where the latent heat flux from the CGCM is higher than the AGCM, which is probably associated with the warm SST bias of the CGCM in that region.

The shortwave radiation patterns were not well reproduced by the global and regional models, in comparison with the ISCCP observations. The SWR from the nested Eta runs is strongly underestimated in the western Atlantic Ocean, which is related to the excessive low cloud coverage in the Eta model in that region. Over the southeastern Atlantic, all models overestimate the SWR, in particular the nested runs, which underestimated the low cloud coverage. According to Carton et al. (2005), this excessive SWR in that region of South Atlantic is due to the deficit in the models of low cloud cover, which maintains the warm SST bias frequently found in CGCMs. Over the continent, the errors of SWR from the nested runs were slightly smaller than the driver models.

Precipitation and SWR from models outputs were compared against the time series of ten PIRATA buoys over the tropical Atlantic Ocean. Although various data gaps were found in the series, in general the version of Eta model nested in the CPTEC CGCM atmospheric conditions generated the smallest errors.

The largest differences between AGCM and CGCM hindcasts occurred over the ocean, where CGCM had smaller errors. This shows that despite the systematic errors in SST, the CGCM is more appropriate for global climate studies. In general, the nested Eta runs improved the hindcasts over the driver models, which are probably due to the regional model resolution and physics.

It was also found that the Eta + C produced better forecasts than Eta + A forecasts. The Eta + C was not benefited from the lower boundary as the predicted SST had larger errors than the persisted SST. However, at the lateral boundary, the CGCM large-scale circulation exhibited smaller errors than the AGCM. In long-term integration of the regional model, the lateral boundary forcing is stronger than the lower boundary forcing as was also found in Chou et al. (2002). Therefore, the better performance of the Eta + C over Eta + A is probably due to the better large-scale forcing description of the CGCM over AGCM.

The evaluation of the ensemble spread versus the RMSE from the global and regional models showed that all models had errors larger than the spread. Tests increasing the number of the members did not increase the spread, therefore the ensemble system cannot be characterized as under-dispersive but that the global model errors need to be reduced before increasing the number of the ensemble members. This characteristic of the global model ensemble is transferred to the regional model.

The results presented so far suggest that the configuration of the Eta nested in the CPTEC CGCM produced best forecasts for the summer season over tropical Atlantic and South America continent. The smallest RMS errors support the added value of dynamical downscaling of the CPTEC GCMs runs with the Eta model, in particular the CGCM. Also, these results suggest the future work of including the full coupling between the regional Eta model and the ocean model at the lower boundary conditions, nested in the CPTEC CGCM in the lateral boundary conditions for improvement of the seasonal forecasts over tropical Atlantic and South America regions.

Acknowledgments The project was funded by the Brazilian Research Council—CNPq under grant no. 480236/07-0 and FAPESP under grant no. 2005/00915-2. The authors thank both CNPq and FAPESP for the grants received for the development of this work, and the TAO Project Office of NOAA/PMEL for the PIRATA data. The authors would like to thank the reviewers' suggestions that helped improving the manuscript.

References

Altshuler E, Fennessy M, Shukla J, Juang H, Rogers E, Mitchell K, Kanamitsu M (2002) Seasonal simulations over North America with a GCM and three regional models. COLA Tech. Rpt. 115. http://www.iges.org/pubs/tech.html

Amengual A, Romero R, Homar V, Ramis C, Alonso S (2007) Impact of the lateral boundary conditions resolution on dynamical downscaling of precipitation in Mediterranean Spain. Clim Dyn 29:487–499. doi:10.1007/s00382-007-0242-0

Antic S et al (2006) Testing the downscaling ability of a one-way nested regional climate model in regions of complex topography. Clim Dyn 26:305–325

Bourlès B, Lumpkin R, Mcphaden MJ et al (2008) The Pirata Program: history, accomplishments, and future directions. Bull Am Meteorol Soc 89:1111–1125. doi:10.1175/2008BAMS2462.1

Carton JA, Chang C-Y, Grodsky S, Nigam S, Wang J (2005) Relationship of the tropical Atlantic to West African rainfall in the NCEP coupled model. In: US Clivar Atlantic Science Conference, Miami, United States

Cavalcanti IFA et al (2002) Global climatological features in a simulation using CPTEC/COLA AGCM. J Clim 15:2965–2988

Chou SC, Nunes AMB, Cavalcanti IFA (2000) Extended range forecasts over South America using the regional Eta model. J Geophys Res 105:10147–10160. doi:10.1029/1999JD901137

Chou SC, Tanajura CAS, Xue Y, Nobre CA (2002) Validation of the coupled Eta/SSiB model over South America. J Geophys Res 107:D20

Chou SC, Bustamante JF, Gomes JL (2005) Evaluation of Eta model seasonal precipitation forecasts over South America. Nonlinear Process Geophys 12:537–555, SRef-ID: 1607-7946/npg/2005-12-537

Chou SC, Marengo JA, Lyra AA, Sueiro G, Pesquero JF, Alves LM, Kay G, Betts R, Chagas DJ, Gomes JL, Bustamante JF, Tavares P (2011) Downscaling of South America present climate driven by 4-member HadCM3 runs. Clim Dyn. doi:10.1007/s00382-011-1002-8

Davey MK, Huddleston M, Sperber KR et al (2002) STOIC: a study of coupled model climatology and variability in tropical oceans regions. Clim Dyn 18:403–420. doi:10.1007/s00382-001-0188-6

Dimitrijevic M, Laprise R (2005) Validation of the nesting technique in a RCM and sensitivity tests to the resolution of the lateral boundary conditions during summer. Clim Dyn 25:555–580

Druyan LM, Fulakeza M, Lonergan P (2002) Dynamic downscaling of seasonal climate predictions over Brazil. J Clim 15:3411–3426

Ek MB, Mitchell KE, Lin Y, Rogers E, Grummen P, Koren V, Gayno G, Tarpley JD (2003) Implementation of NOAH land surface advances in the National Centers for Environmental Prediction operational mesoscale Eta model. J Geophys Res 108:D22–D8851. doi:10.1029/2002JD003246

Fels SB, Schwarzkopf MD (1975) The simplified exchange approximation: a new method for radiative transfer calculations. J Atmos Sci 32:1475–1488. doi:10.1175/1520-0469

Fennessy MJ, Shukla J (2000) Seasonal prediction over North America with a regional model nested in a global model. J Clim 13:2605–2627. doi:10.1175/1520-0442

Ferrier BS, Lin Y, Black T, Rogers E, DiMego G (2002) Implementation of a new grid-scale cloud and precipitation scheme in the NCEP Eta model. In: 15th Conference on numerical weather prediction, Am Meteorol Soc

Frey H, Latif M, Stockdale T (1997) The coupled GCM ECHO-2. Part I: the tropical Pacific. Mon Weather Rev 125:703–720

Harshvardhan RD, Randall DA, Corsetti TC (1987) A fast radiation parametrization for atmospheric circulation models. J Geophys Res 92:1009–1016. doi:10.1029/JD092iD01p01009

Hu Z-Z, Huang B, Hou Y-T (2011) Sensitivity of tropical climate to low-level clouds in the NCEP climate forecast system. Clim Dyn 36:1795–1811. doi:10.1007/s00382-010-0797-z

Huang B, Hu Z-Z, Jha B (2007) Evolution of model systematic errors in the Tropical Atlantic Basin from coupled climate hindcasts. Clim Dyn 28:661–682. doi:10.1007/s00382-006-0223-8

Janjic ZI (1994) The step-mountain Eta coordinate model: further developments of the convection, viscous sublayer and turbulence closure schemes. Mon Weather Rev 122:927–945. doi:10.1175/1520-0493

Juang H-M, Kanamitsu M (1994) The NMC nested regional spectral model. Mon Weather Rev 122:3–26

Kalnay E, Kanamitsu M, Kistler R et al (1996) The NCEP/NCAR 40-year reanalysis project. Bull Am Meteorol Soc 77:437–471. doi:10.1175/1520-0477

Katsafados P, Papadopoulos A, Kallos G (2005) Regional atmospheric response to tropical Pacific SST perturbations. Geophys Res Lett 32:L04806. doi:10.1029/2004GL021828

Kuo HL (1974) Further studies of the parameterization of the influence of cumulus convection on large scale flow. J Atmos Sci 31:1232–1240

Lacis AA, Hansen JE (1974) A parameterization of absorption of solar radiation in the earth's atmosphere. J Atmos Sci 31:118–133

Laprise R, Elía R, Caya D, Biner S, Lucas-Picher P, Diaconescu E, Leduc M, Alexandru A, Separovic L (2008) Challenging some tenets of regional climate modelling. Meteorol Atmos Phys 100:3–22. doi:10.1007/s00703-008-0292-9

Lin JL (2007) The double-ITCZ problem in IPCC AR4 coupled GCMs: ocean–atmosphere feedback analysis. J Clim 20:4497–4525

Lobocki L (1993) A procedure for the derivation of surface-layer bulk relationships from simplified second order closure models. J Appl Meteorol 32:126–138

Luo JJ et al (2005) Reducing climatology bias in an ocean–atmosphere CGCM with improved coupling physics. J Clim 18:2344–2360

Mechoso CR (2006) Modeling the south eastern Pacific climate: Progress and challenges. NCEP EMC seminar. http://www.emc.ncep.noaa.gov/seminars/presentations/2006/Mechoso.NCEP.Jan.06.ppt

Mellor GL, Yamada T (1982) Development of a turbulence closure model for geophysical fluid problems. Rev Geophys Phys Space Phys 20:851–875

Mesinger F (1984) A blocking technique for representation of mountains in atmospheric models. Riv Meteorol Aeronaut 44:195–202

Misra V, Dirmeyer PA, Kirtman BP (2003) Dynamic downscaling of regional climate over South America. J Clim 16:103–117

Moorthi S, Suarez MJ (1992) Relaxed Arakawa-Schubert: a parameterization of moist convection for general circulation models. Mon Weather Rev 120:978–1002

Nobre P, Moura AD, Sun L (2001) Dynamical downscaling of seasonal climate prediction over Nordeste Brazil with NCEP's regional spectral model at IRI. Bull Am Meteorol Soc 82:2787–2796

Nobre P, Malagutti M, Giarolla E (2006) Coupled Ocean–atmosphere Variability of the South American Monsoon System. Comm. 8th Conference on Southern Hemisphere Meteorology and Oceanography, Proceedings of the 8th Comm. on Southern Hemisphere Meteorology and Oceanography, Foz do Iguaçú, Brazil

Nobre P, Malagutti M, Urbano DF, Almeida RAF, Giarolla E (2009) Amazon deforestation and climate change in a coupled model simulation. J Clim 22:5686–5697

Pacanowski RC, Griffies SM (1998) MOM 3.0 Manual. NOAA/Geophysical Fluid Dynamics Laboratory. Princeton, United States

Paulson CA (1970) The mathematical representation of wind speed and temperature profiles in the unstable atmospheric surface layer. J Appl Meteorol 9:857–861

Pesquero JF, Chou SC, Nobre CA, Marengo JA (2010) Climate downscaling over South America for 1961–1970 using the Eta model. Theor Appl Climatol 99:75–93. doi:10.1007/s00704-009-0123-z

Pezzi LP, Cavalcanti IFA (2000) Testes de sensibilidade usando-se dois esquemas diferentes de convecção, (Sensitivity analysis using two different convection schemes in the CPTEC/COLA AGCM). Comm. 11th Brazilian Conference of Meteorology, Proceedings of the 11th Brazilian Conference of Meteorology, Rio de Janeiro, Brazil

Pope V, Gallani M, Rowtree P, Stratton R (2000) The impact of new physical parameterizations in the Hadley Centre climate model. Clim Dyn 16:123–146

Rao VB, Hada K (1990) Characteristics of rainfall over Brazil: annual variations and connections with the Southern Oscillation. Theor Appl Climatol 42:81–91

Rauscher SA, Seth A, Liebmann B, Qian J-H, Camargo SJ (2007) Regional climate model–simulated timing and character of seasonal rains in South America. Mon Weather Rev 135:2642–2657

Reynolds RW, Smith TM (1994) Improved global sea surface temperature analyses using optimum interpolation. J Clim 7:929–948

Reynolds RW, Rayner NA, Smith TM, Stokes DC, Wang W (2002) An improved in situ and satellite SST analysis for climate. J Clim 15:1609–1625

Richter I, Xie SP (2008) On the origin of equatorial Atlantic biases in coupled general circulation models. Clim Dyn 30:587–598

Rosati A, Miyakoda K (1988) A general circulation model for upper ocean simulation. J Phys Oceanogr 18:1601–1626

Schneider EK (2002) Understanding differences between the equatorial Pacific as simulated by two coupled GCMs. J Clim 15:449–469

Seluchi ME, Chou SC (2000) Ajuste del esquema convectivo de betts-miller en el modelo Eta/CPTEC. Comm. 11th Brazilian Conference of Meteorology, Proceedings of the 11th Brazilian Conference of Meteorology, Rio de Janeiro, Brazil

Seth A et al (2007) RegCM3 regional climatologies for South America using reanalysis and ECHAM global model driving fields. Clim Dyn 28:461–480

Shukla J (1981) Dynamical predictability of monthly means. J Atmos Sci 38:2547–2572

Silva AR (2009) The life cycle of the South American monsoon system: observation and simulation. PhD thesis, National Institute for Space Research

Solman SA, Nuñez MN, Cabré MF (2008) Regional climate change experiments over southern South America. I: present climate. Clim Dyn 30:533–552

Xue Y, Zeng FJ, Mitchell KE, Janjic Z, Rogers E (1991) The impact of land surface processes on simulations of the U.S. hydrological cycle: a case study of the 1993 flood using the SsiB Land Surface Model in the NCEP Eta Regional Model. Mon Weather Rev 129:2833–2860

Zhang GJ, Wang H (2006) Toward mitigating the double ITCZ problem in NCAR CCSM3. Geophys Res Lett 33:L06709